encit 2020

ABCM Associação Brasileira de Engenharia e Ciências Mecânicas

18th Brazilian Congress of Thermal Sciences and Engineering
November 16–20, 2020 (Online)

ENCIT-2020-0197
LINEAR STABILITY ANALYSIS OF NON-NEWTONIAN FREE SURFACE FLOWS: A MATHEMATICAL STUDY ON THE TEMPORAL AND SPATIAL BRANCHES

Valdirene da Rosa Rocho
Guilherme Henrique Fiorot
Sergio Viçosa Möller
valdirenerocho@gmail.com
guilherme.fiorot@ufrgs.br
svmoller@ufrgs.br
Programa de Pós-Graduação em Engenharia Mecânica - PROMEC
Universidade Federal do Rio Grande do Sul - UFRGS

Abstract. *Free surface fluid flow may eventually present itself in sufficient conditions for certain hydrodynamic instabilities to appear. These instabilities are called roll waves and are hydrodynamic structures that propagate along with the flow, with constant velocity and amplitude. In this scenario, it is necessary to understand how the roll waves evolution occurs in order to control and predict the flow behavior. In this work, a theoretical approach was conducted using stability analysis to the mathematical model. The flow modeling was based on the Cauchy equations, with the Herschel-Bulkley rheological model inserted in the viscous part of the tension tensor. The objective of this work was to perform linear stability analysis and obtain information on the temporal and spatial branches of the solution obtained for the dispersion equation* $D(\omega,\ k) = 0$ *of the problem. It was mathematically demonstrated that the instability criteria can be defined through the minimum Froude number (*F_{min}*) and Froude number on the singularity point (*F_s*), which retrieves solutions from the literature. In addition, this work explored the results for a Herschel-Bulkley type of fluid and evidenced asymptotic characteristics of the growth rates and wave propagation velocity of instabilities for long waves (*$k \to 0$*) and short waves (*$k \to +\infty$*).*

Keywords: *Free surface flow, roll waves, Herschel-Bulkley, stability analysis.*

1. INTRODUCTION

The theory of hydrodynamic instability has been gaining prominence in fluid mechanics since the times of Osborne Reynolds, who developed the famous experiment on the instability of laminar flow in a tube, and can be considered the fundamental experiment in the study of hydrodynamic instabilities (Charru, 2011). These instabilities arise in the proximity of the uniform regime established by flow in an attempt to balance the active forces - body or field forces and surface forces, with the resistive forces, usually associated with viscous friction and arising from the physical and rheological properties of the flowing fluid.

More specifically, the propagation of those instabilities in free surface flows which are representative of many natural geophysical flows, have significant importance from the Engineering point of view. In this case, when instabilities present sufficient conditions to developed and stabilize, they received the name of roll waves. Modeling the roll waves instability development is a difficult task that can become even more complicated when fluids present non-Newtonian rheological behavior (Liu, 1994; Di Cristo *et al.*, 2010; Fiorot, 2012; Fer *et al.*, 2002).

Non-Newtonian fluids feature non-linear relationship between strain rate and shear stress, which demands ore than one parameter to define the viscous behavior of the fluid, opposing to Newtonian fluids. There are many examples of fluids of this type: paints, solutions of various polymers, oil in water, fibers in liquid paper pulp, aqueous mixtures of granular solid material (mud, for example), among others; where one can find the relevance of the presence of roll waves instabilities in flows.

Theoretically, the roll wave study aims to examine the necessary conditions for instabilities to grow in time and space. Researchers usually establish the criteria for the generation and propagation of instabilities, which are dependent on the Froude number. The first recognised use of a theoretical roll waves study was conducted for shallow water flow in open channels by Jeffreys (1925) as a problem of linearized instability in a turbulent current. Following this, the mathematical theory for finite amplitude roll waves was later given by Dressler (1949), who described that for given values of slope

and roughness, it is also necessary to specify the wave propagation velocity and wavelength to determine the remaining flow characteristics, such as wave amplitude, flow velocity and depth. Furthermore, Dressler also found that roll waves will only occur if the roughness of the channel bed is above zero, but less than a certain critical value, as required by the instability criterion for a linearized perturbation. This study was later extended by Needham and Merkin (1984), Di Cristo *et al.* (2010), and Balmforth and Mandre (2004), and also adapted for laminar flows (Ishihara *et al.*, 1954), and non-Newtonian fluids by (Liu, 1994; Ng and Mei, 1994; Maciel *et al.*, 2013), among others.

Thus, this work arise with the motivation and the objective to, at first, reevaluate the specific case in the literature of Maciel *et al.* (2013) and detail the stability solution in limit cases, with the purpose of better understand and improved the understanding of the problem and the validity of the modeling. Moreover, the present work conducted spatial linear stability analysis on the system of equations governing the problem to obtain additional information on the temporal and spatial branches.

2. METHODOLOGY

To the carry out this work, the mathematical model based on the Cauchy equations was used with the Herschel-Bulkley rheological model into the viscous part of the stress tensor.

2.1 Rheological model

Aqueous mixtures of cohesive solid particle represent countless types of industrial and natural fluids. To represent such complex type of fluid, the three-parameter Herschel-Bulkley rheological model is well qualified to represent the shearing behavior, and under steady conditions and simple shear, can be written as to Eq. (1):

$$\begin{aligned} &\tau_{xz} = \tau_c + K_n \left(\frac{\partial u}{\partial z}\right)^n, \ \text{if } \tau_{xz} > \tau_c \\ &\frac{\partial u}{\partial z} = 0, \ \text{if } \tau_{xz} < \tau_c, \end{aligned} \tag{1}$$

where τ_{xz} is the shear stress acting in the direction x due to a gradient in z, u the velocity component in the direction x, z the vertical coordinate, $\partial u/\partial z$ the strain or shear rate, τ_c the limit flow stress, K_n the fluid consistency index and n the fluid flow index.

2.2 Free-surface flow

In non-Newtonian fluid flow, the driving equations of the phenomenon are obtained from the Cauchy system of equations, according is presented by Liu (1994), Ng and Mei (1994) among others. For the specific case of a Herschel-Bulkley type fluid, it can be assume the following hypotheses (Maciel *et al.*, 2013):

- Homogeneous muddy fluid, of Herschel-Bulkley rheological behavior and incompressible, therefore the specific mass (ρ) is constant;
- Shallow water conditions, i.e., flow depth (h) much smaller than the characteristic longitudinal length (L) and the width of the channel (l);
- Flow occurs mainly by the action of gravity, in a laminar regime;
- Fixed channel bottom;

and the following boundary conditions for the mathematical model:

- Kinematic conditions on the free surface: $w(x,\ z,\ t) = \dfrac{\partial h}{\partial t} + u\dfrac{\partial h}{\partial x}$ to $z = h(x,\ t)$;
- Impermeability conditions in the bottom: $u(x,\ z,\ t) = w(x,\ z,\ t) = 0$ for $z = 0$;
- Stresses on the free surface and bottom of the channel: $P(z) = 0$ and $\tau_{xz} = 0$ to $z = h(x,\ t)$, $\tau_{xz}(z) = \tau_f$ to $z = 0$,

where w is the velocity component in the direction z, P is the pressure, τ_f is the shear stress at the bottom of the channel and t represents time.

In order to evaluate the problem in a physical and mathematical mode, the system of equations that govern this flow is rewritten, applying the boundary conditions and, subsequently, transformed into dimensionless variables. For this process, the scales of the various parameters must be chosen appropriately to provide coefficients that can represent proportions between the flow characteristics. The scales were chosen as follows:

- Length scale: $x^* = {}^{x}/_{L}$ and $(h^*,\ z^*) = {}^{(h,\ z)}/_{h_0}$;
- Velocity scales: $u^* = {}^{u}/_{u_0}$;
- Time scale: $t^* = {}^{u_0 t}/_{L}$;
- Froude number: $F = {}^{u_0}/_{\sqrt{g h_0 \cos\theta}}$ e
- Dimensionless yield stress: $C = {}^{\tau_c}/_{\rho g h_0 \sin\theta}$.

Stands out that the sub-indices $(\ )_0$ indicate the uniform flow conditions and $(\ )^*$ the asterisks represent the dimensionless variables, which will be omitted in the following equations. Introducing them in the equations we have the following system:

- Continuity equation:

$$\frac{\partial h}{\partial t} + \frac{\partial (hu)}{\partial x} = 0. \tag{2}$$

- Motion quantity equation:

$$h\left(\frac{\partial u}{\partial t} + \alpha u \frac{\partial u}{\partial x}\right) + \frac{h}{F^2}\frac{\partial h}{\partial x} + (1-\alpha)u\frac{\partial h}{\partial t} = h - C - (1-C)\left[hu\frac{(1-C)\,(n+1+nC)}{(h-C)\,(nh+h+nC)}\right]^n, \tag{3}$$

where,

$$\alpha = \left(\frac{2n+1}{3n+2}\right)\frac{2\,(n+1)^2\,h_0 + n\,(4n+3)\,C}{(n+1)^2\,h_0 + 2n\,(n+1)\,C + \frac{n^2 C^2}{h_0}}. \tag{4}$$

From the mathematical model determined in dimensionless variables, it is possible to seek favorable conditions for the formation of instabilities.

2.3 Linear Stability Analysis

In search of the flow stability conditions, a linear stability analysis if done on the system of equations that represent the problem (Eq. (2) and (3)). When performing such analysis, it is necessary to search for information on how instabilities are propagated namely: the growth rate, and the propagation velocity.

For such analysis, an infinitesimal perturbation of small amplitude is added to the uniform flow $(h,\ u) = (1,\ 1)$, which is given by:

$$h(x,\ t) = 1 + \widehat{H}(x,\ t) \quad \text{and} \quad u(x,\ t) = 1 + \widehat{U}(x,\ t) \tag{5}$$

when applying them in the system of equations, the same becomes:

$$\frac{\partial \widehat{H}}{\partial t} + \frac{\partial \widehat{U}}{\partial x} + \frac{\partial \widehat{H}}{\partial x} = 0 \tag{6}$$

and

$$\frac{\partial \widehat{U}}{\partial t} + \alpha\frac{\partial \widehat{U}}{\partial x} + \frac{1}{F^2}\frac{\partial \widehat{H}}{\partial x} + (1-\alpha)\frac{\partial \widehat{H}}{\partial t} = 1 + \widehat{H} - C - (1-C)\left[\left(1+\widehat{H}\right)\left(1+\widehat{U}\right)\cdot \right.$$
$$\left. \cdot\frac{(1-C)\,(n+1+nC)}{\left(1+\widehat{H}-C\right)\left[(n+1)\left(1+\widehat{H}\right)+nC\right]}\right]^n. \tag{7}$$

Deriving the equation Eq. (6) in relation to the variable x and t, and the Eq. (7) in relation to the variable x, and then replacing the derivatives resulting from Eq. (6) in the derivative of Eq. (7), and after some algebraic manipulations, we obtain the following expression (Eq. (8)):

$$\frac{\partial^2 \widehat{H}}{\partial t^2} + \left(\alpha - \frac{1}{F^2}\right)\frac{\partial^2 \widehat{H}}{\partial x^2} + 2\alpha\frac{\partial^2 \widehat{H}}{\partial t \partial x} + n(1-C)\frac{\partial \widehat{H}}{\partial t} + \frac{(n+1)\,(2n+1)}{(nC+1+n)}\frac{\partial \widehat{H}}{\partial x} = 0. \tag{8}$$

It is assumed that the solution of Eq. (8) is of the type (Liu, 1994; Di Cristo and Vacca, 2005; Maciel *et al.*, 2013):

$$\widehat{H}(x,\ t) = \left|\widehat{H}\right| e^{i(\omega t - kx)} \tag{9}$$

being $\left|\widehat{H}\right|$ the magnitude of the perturbation, k and ω are the wavenumber and the frequency, respectively. Following the classical linear stability theory, these are decomposed into elementary waves with $k = k_r + ik_i$, the complex wavenumber, and $\omega = \omega_r + i\omega_i$, complex frequency. Assuming the solution given by Eq. (9) and inserting it in Eq. (8), results in the quadratic dispersion equation displayed by Eq. (10).

$$D(\omega,\ k,\ n,\ \alpha,\ C,\ F) = \omega^2 + k^2\left(\alpha - \frac{1}{F^2}\right) - 2\alpha k\omega - i\vartheta\omega + i\varphi k = 0 \tag{10}$$

with

$$\varphi = \frac{(n+1)\,(2n+1)}{(n+1+nC)} \quad \text{and} \quad \vartheta = n\,(1-C)\,. \tag{11}$$

General mathematical criteria based on the dispersion relation properties $D(\omega,\ k,\ n,\ \alpha,\ C,\ F) = 0$ (Eq. 10) in the complex plane k and ω can be derived to determine the nature of the instability. From this equation, we can observe the temporal evolution of small perturbation through the branches ω, taking the consideration of $k = k_r$, with $k_i = 0$, from which ω_i indicates an amplification in time. Another possibility is to observe the spatial evolution of the instability, making the consideration that $\omega = \omega_r$, with $\omega_i = 0$, and from the solution, get k_i which is the spatial amplification rate of the instabilities (Briggs, 1964; Huerre and Monkewitz, 1990).

It is intended here to reevaluate such analyzes already promoted in the literature (Maciel *et al.*, 2013; Ferreira, 2013), and to observe the growth rates of instabilities and wave propagation velocities, as will be shown. The entire mathematical procedure will be considered as a result of this work.

3. RESULTS

3.1 Temporal stability analysis

To deduce the analytical temporal solution of the problem represented by the dispersion equation (Eq. (10)), it is assumed that $k = k_r$, and solve the Eq. (10) for ω. Thus, the solution obtained, called the temporal branch, is given by the Eq. (12),

$$\omega_{\pm}(k) = \alpha k + \frac{\vartheta i}{2} \pm \sqrt{k^2\left(\alpha^2 - \alpha + \frac{1}{F^2}\right) + ik\,(\alpha\vartheta - \varphi) - \frac{\vartheta^2}{4}}. \tag{12}$$

In other words, the temporal modes $\omega_{\pm}(k)$ refer to cases where the complex frequency ω is determined as a function of the number of real waves k (Briggs, 1964; Huerre and Monkewitz, 1990). The existence of instabilities is represented by the imaginary part of the branches $\omega_{\pm}(k)$, composing the temporal rate the through of spatial perturbation, and for this problem it is expressed as follows:

$$Im\left\{\omega_{\pm}(k)\right\} = \frac{\vartheta}{2} \pm \frac{1}{4}\sqrt{-8k^2\left(\alpha^2 - \alpha + \frac{1}{F^2}\right) + 2\vartheta^2 + 8\sqrt{\left[k^2\left(\alpha^2 - \alpha + \frac{1}{F^2}\right) - \frac{\vartheta^2}{4}\right]^2 + (k\alpha\vartheta - k\varphi)^2}}. \tag{13}$$

In this way, the disturbance amplification occurs when $Im\{\omega_{\pm}(k)\} < 0$. Then, it is verified $Im\{\omega_{\pm}(k)\} = 0$ to find the stability criterion as function of the variable F. Thus, a necessary condition of a favorable domain is obtained for the formation of instabilities in the flow free surface given by Eq. (14):

$$F > F_{\min} = \frac{\vartheta}{\sqrt{\vartheta^2\alpha - 2\alpha\vartheta\varphi + \varphi^2}}. \tag{14}$$

Through this temporal linear stability analysis, a control parameter F is identify, where it can be determined a minimum Froude number, $F_{\min}$, above which instabilities will be amplified in this system. In order to explore this control parameter, Fig. 1 illustrates the growth rate of the perturbation ω_i as a function of the real wavenumber k for the branches temporal. We fixed the parameters $C = 0.3$ and $n = 1/3$ and the Froude number was varied.

It can be seen in Fig. 1 that two temporal branches coexist for different Froude numbers, which occurs due to the quadratic characteristic of the dispersion equation (Eq. (10)). It is also noted the disturbance amplification for $F > F_{\min}$ and $k > 0$. Observing the graphs, it is perceive that $\omega_{i,\pm}$ has asymptotic behaviors when $k \to 0$ and $k \to \infty$. To investigate the behavior of $\omega_{i,\pm}$ in these values, we first sought the maximum and minimum values of the temporal growth. Applying the derivation to Eq. (13) as function of k, a critical point of the function is determined, which occurs when $k = 0$. Replacing it again in Eq. (13), it is possible to obtain the maximum and minimum value for each temporal branch (growth rate), where:

$$\omega_{i,\max} = \frac{\vartheta}{2} + \frac{1}{4}\sqrt{2\vartheta^2 + 2\vartheta^2} = \frac{\vartheta}{2} + \frac{\vartheta}{2} = \vartheta \tag{15}$$

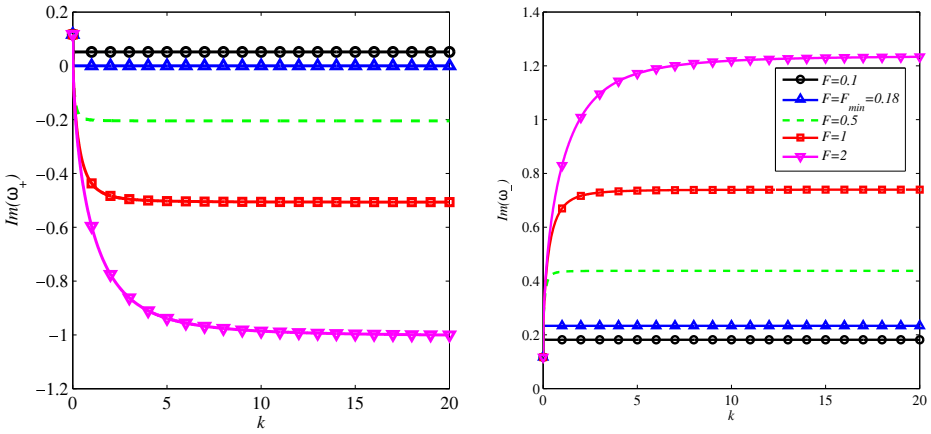

(a) Positive branches. (b) Negative branches.

Figure 1. Growth rate of perturbations for a Herschel-Bulkley fluid at various Froude numbers.

is the maximum value of the positive temporal branch, and

$$\omega_{i,\min} = \frac{\vartheta}{2} - \frac{1}{4}\sqrt{2\vartheta^2 + 2\vartheta^2} = \frac{\vartheta}{2} - \frac{\vartheta}{2} = 0 \tag{16}$$

is the minimum value of the negative temporal branch.

Still, it is observed that according to Fig. 1, the amplification rate is asymptotic when $k \to +\infty$, which can be calculated from the limit:

$$\lim_{k\to+\infty} Im\{\omega_{\pm}(k)\} = \frac{\vartheta}{2} \pm \frac{1}{2}\frac{(\alpha\vartheta - \varphi)}{\sqrt{\alpha^2 - \alpha + \frac{1}{F^2}}} \tag{17}$$

Asymptotic growth rates are valid for Froude numbers above the minimum value ($F > F_{min}$). Thus, from a geometric analysis (Fig. 1) and comparative of the results found (Eq. 13), the limit values found were validated in the Eq. (15), (16) and (17).

Another important parameter that needs to be considered for this analysis is the wave propagation velocity (also called group velocity), which is calculated from the real part of the branches $\omega_{\pm}(k)$, that is,

$$U = \frac{Re\{\omega_{\pm}(k)\}}{k} \tag{18}$$

where,

$$Re\{\omega_{\pm}(k)\} = \alpha k \pm \frac{1}{4}\sqrt{8k^2\left(\alpha^2 - \alpha + \frac{1}{F^2}\right) - 2\vartheta^2 + 8\sqrt{\left[k^2\left(\alpha^2 - \alpha + \frac{1}{F^2}\right) - \frac{\vartheta^2}{4}\right]^2 + (k\alpha\vartheta - k\varphi)^2}}, \tag{19}$$

which can be seen in Fig. 2.

From the Fig. 2, it is note that the variation of the Froude number implies in the reduction of the wave propagation velocity U. And still, we notice the reduction of U as the wavenumber increases, and from the a certain value for k the velocity becomes constant.

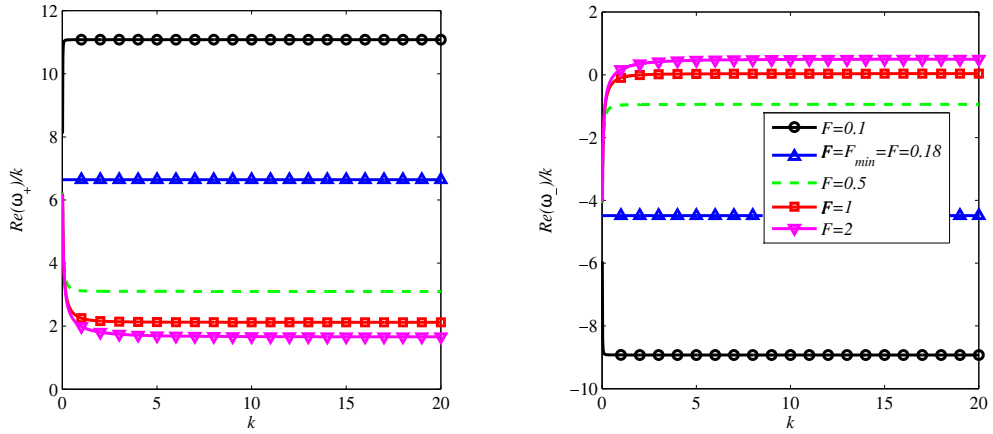

(a) Positive branches. (b) Negative branches.

Figure 2. Propagation velocity of perturbations for a Herschel-Bulkley fluid at various Froude numbers.

In the same context as the growth rate, we can estimate asymptotic values for the propagation velocity, which can be observed in Fig. 2. For long waves, that is, $k \to 0$, we have the limit value given by

$$U = \lim_{k\to 0} \frac{Re\{\omega_{\pm}(k)\}}{k} = \alpha \pm \frac{(\alpha\vartheta - \varphi)}{\vartheta}, \tag{20}$$

and for short waves, that is, $k \to +\infty$, the asymptotic value of the propagation velocity is given by

$$U = \lim_{k\to +\infty} \frac{Re\{\omega_{\pm}(k)\}}{k} = \alpha \pm \sqrt{\alpha^2 - \alpha + \frac{1}{F^2}}. \tag{21}$$

It is worth mentioning that, from the Eq. (20) and (21), U assumes different dependency relations with the flow parameters. The Fig. 3 brings this information considering only the positive branch, placing the propagation speed as a function of F, for values of k fixed. We emphasize that the horizontal axis limits were fixed for waves in the domain of favorable amplification $(F > 0.18)$ and that, for large numbers of Froude, the physical meaning can be lost.

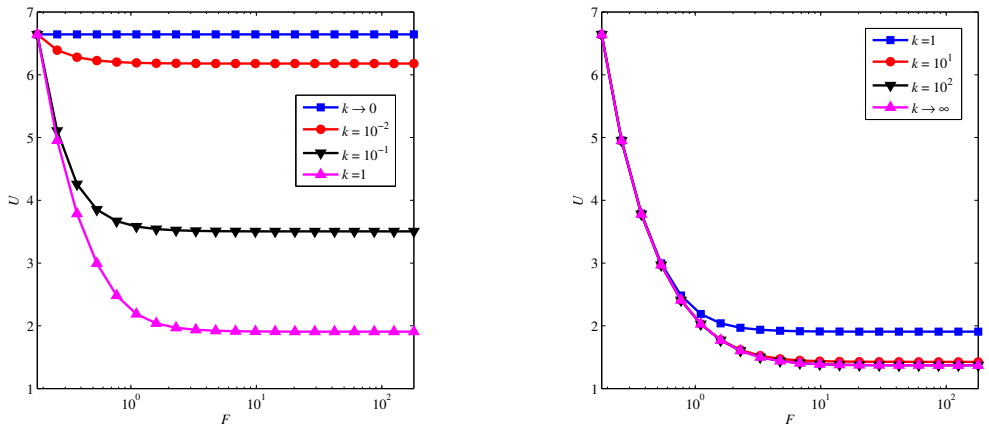

(a) Wave propagation speed for $k \to 0$. (b) Wave propagation speed for $k \to \infty$.

Figure 3. Wave propagation velocity as a function of the F for different wavenumbers for a Herschel-Bulkley fluid.

The Fig. 3 shows that U is strongly dependent on the Froude number, mainly for high wavenumber. For $k \to 0$, the influence of F is increasingly smaller, until it becomes null. It is also noticed that the behavior is not linear, and that there is a limit value of F for which the waves propagate at a constant speed. In fact, if we also consider that $F \to \infty$, then we have $U(k \to \infty) = \alpha + \sqrt{\alpha^2 - \alpha}$, which it can still be confirmed through Fig. 3.

3.2 Spatial stability analysis

The spatial modes $k_{\pm}(\omega)$ refer to cases in which the wavenumber complex k is determined as a function of the frequency ω. The existence of instabilities is represented by the imaginary part of the branches $(Im\{k_{\pm}(\omega)\})$ obtained by

solving Eq. (10) for the number of complex waves k when ω is given real ($\omega = \omega_r$). When $Im\{k_\pm(\omega)\} > 0$, infinitesimal perturbations would be amplified in space. From this logic, one obtains:

$$k_\pm(\omega) = \frac{2\alpha\omega - \varphi i \pm \sqrt{4\omega^2\left(\alpha^2 - \alpha + \frac{1}{F^2}\right) + 4\omega i\left(\alpha\vartheta - \alpha\varphi - \frac{\vartheta}{F^2}\right) - \varphi^2}}{2\left(\alpha - \frac{1}{F^2}\right)}. \tag{22}$$

Similarly to the temporal stability analysis, we sought the spatial instability growth rate, $Im\{k_\pm(\omega)\}$, and the wave propagation velocity, given from of $Re\{k_\pm(\omega)\}$, which are represented by Eq. (23) and (24), respectively.

$$Im\{k_\pm(\omega)\} = \frac{-\varphi \pm \sqrt{\frac{\sqrt{\left(4\omega^2\left(\alpha^2-\alpha+\frac{1}{F^2}\right)-\varphi^2\right)^2+\left(4\omega\left(\alpha\vartheta-\alpha\varphi-\frac{\vartheta}{F^2}\right)\right)^2}-4\omega^2\left(\alpha^2-\alpha+\frac{1}{F^2}\right)+\varphi^2}{2}}}{2\left(\alpha - \frac{1}{F^2}\right)}, \tag{23}$$

$$Re\{k_\pm(\omega)\} = \frac{2\alpha\omega \pm \sqrt{\frac{\sqrt{\left(4\omega^2\left(\alpha^2-\alpha+\frac{1}{F^2}\right)-\varphi^2\right)^2+\left(4\omega\left(\alpha\vartheta-\alpha\varphi-\frac{\vartheta}{F^2}\right)\right)^2}+4\omega^2\left(\alpha^2-\alpha+\frac{1}{F^2}\right)-\varphi^2}{2}}}{2\left(\alpha - \frac{1}{F^2}\right)}. \tag{24}$$

When evaluating the Eq. (23) and (24), it is noticed that both have a singularity point. Then, we analyzed when $Im\{k_\pm(\omega)\} = 0$ for the variable F to determine it the singularity point, given by Eq. (25):

$$F_s = \frac{1}{\sqrt{\alpha}}. \tag{25}$$

From Eq. (23) and (24) we can confirm that F_{min} takes the form previously reached in Eq. (14).

Seeking out to analyze the spatial growth rates as a function of frequency, numerical tests were performed for different F, keeping the same non-Newtonian fluid characteristics and considering the parameters $C = 0.3$ and $n = 1/3$, which are illustrated in Fig. 4.

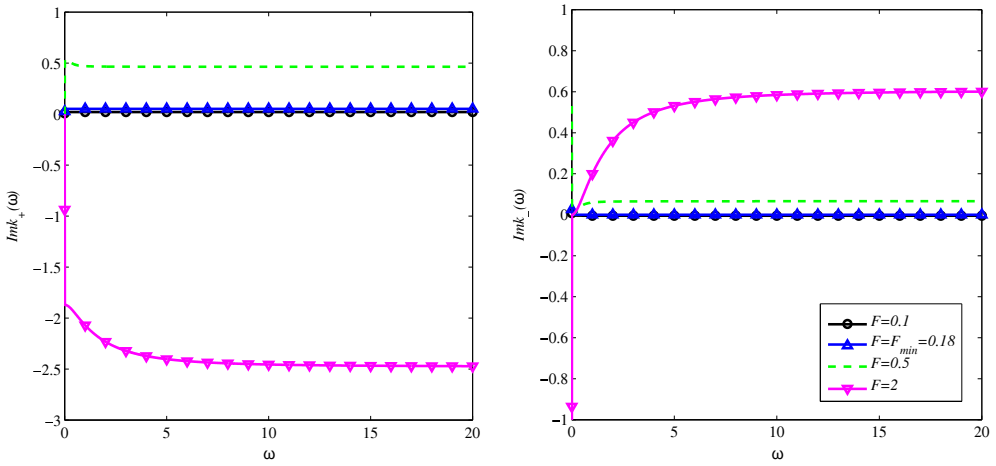

(a) Positive branches. (b) Negative branches.

Figure 4. Growth rate of perturbations for a Herschel-Bulkley fluid at various Froude numbers.

It can be seen in the Fig. 4 that for $F > F_{min}$ at least one of the the space branches show susceptible positive values, meaning there is amplification of perturbations in space. Close to the singularity point ($F_s = 0.9628$), In the calculations, it was noticed that for values of F close to the singularity, the growth rate presented values which tended to infinity, and therefore were not represented in Fig. 4. Still, far from F_s, it is noticed that both branches are presented in favorable configuration $Im\{k_\pm(\omega) > 0\}$ when $F_{min} < F < F_s$, and that the space branch positive (Fig. 4 (a)) changes its signal for $F > F_s$, therefore pointing out the evanescence of the perturbations in that direction.

Based on the two established conditions (F_{min} and F_s), we performed numerical tests to evaluate the behavior of the function $Im\{k_\pm(\omega)\}$, in the vicinity of the singularity point. In Fig. 5, the spatial growth rate is plotted as a function of ω for F close to F_s singularity, as performed in Ferreira (2013).

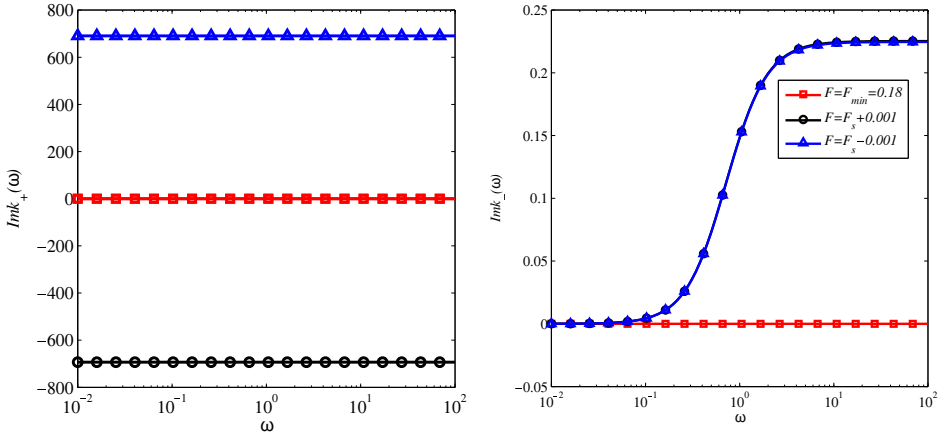

(a) Positive branches. (b) Negative branches.

Figure 5. Growth rate of perturbations for a Herschel-Bulkley fluid ($C = 0.3$ and $n = 1/3$) in vicinity of $F_s = 0.9638$.

Through Fig. 5 it is highlighted the change in the spatial growth rate produced by F_s. In the positive branch Fig. 5 (a): for F slightly higher than F_s, $Im\{k_+(\omega)\} < 0$ (stability, no amplification); for F slightly smaller than F_s, $Im\{k_+(\omega)\} > 0$ (instability, amplification). In the Fig. 5 (b), the negative branch, for every value for ω, the spatial growth rate is positive $Im\{k_-(\omega)\} > 0$.

Another identified feature of $Im\{k_+(\omega)\}$ is the asymptotic behavior when $\omega \to +\infty$ (short waves) that was determined by as shows Eq. (26),

$$\lim_{\omega\to+\infty} Im\{k_\pm(\omega)\} = -\frac{\varphi}{2\left(\alpha - \frac{1}{F^2}\right)} \pm \frac{\left(\alpha\vartheta - \alpha\varphi - \frac{\vartheta}{F^2}\right)}{2\left(\alpha - \frac{1}{F^2}\right)\sqrt{\alpha^2 - \alpha + \frac{1}{F^2}}}. \tag{26}$$

Again, the wave propagation velocity now defined as:

$$U = \frac{\omega}{Re\{k_\pm(\omega)\}}, \tag{27}$$

is calculated and plotted in Fig. 6 which illustrates its dependency on ω for different F.

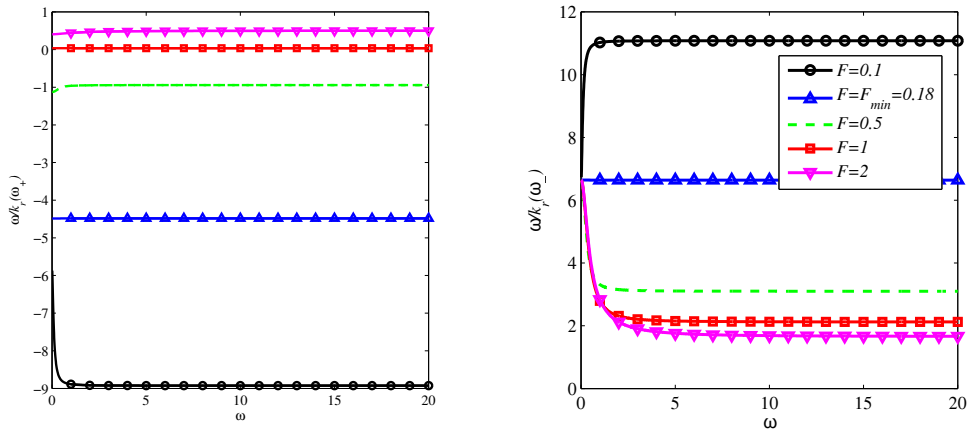

(a) Positive branches. (b) Negative branches.

Figure 6. Propagation velocity of perturbations for a Herschel-Bulkley fluid at various Froude numbers.

In Fig. 6 it is observed that when $F > F_{min}$, U has practically constant values for the positive branches (Fig. 6 (a)). Once again, it can be noticed the signal variation showed by the positive branch for which $U < 0$ when $F_{min} < F < F_s$, and $U > 0$ when $F > F_s$. The positive branch also show $U \to 0$ when $F \to F_s$. The same is not true for the negative branch (Fig. 6 (b)), where $U > 0$ for any $F > F_{min}$.

Still in question of behavior, it can be observed in Fig. 6 that the curves have asymptotic behavior when the frequency

$\omega \to +\infty$. Thus, by means of the limit operation:

$$U = \lim_{\omega \to +\infty} \frac{\omega}{Re\{k_{\pm}(\omega)\}} = \frac{\alpha - \frac{1}{F^2}}{\alpha \pm \sqrt{\alpha^2 - \alpha + \frac{1}{F^2}}}. \tag{28}$$

Comparing Eq. (28) with Eq. (21), it is noticed that U assumes a different dependency relation with the flow parameters. The Fig. 7 brings this information considering only the negative branch, placing the propagation velocity as a function of F, for values of ω fixed and $F > F_{min}$.

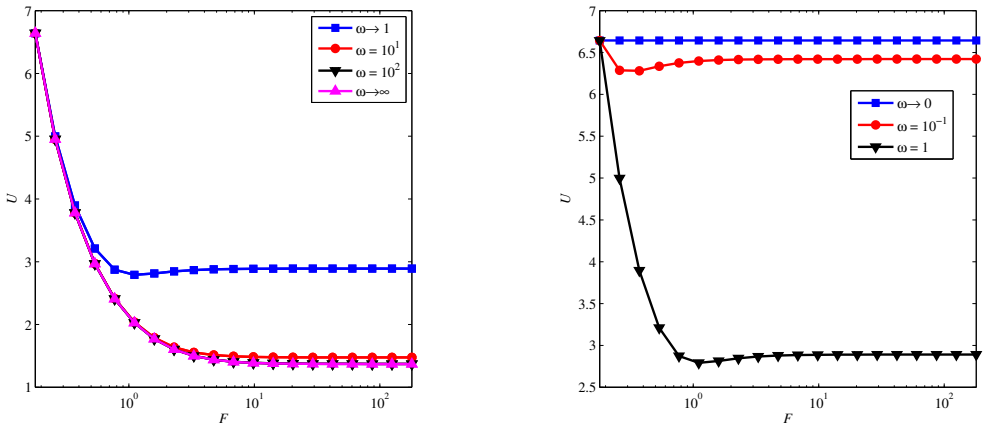

(a) Wave propagation velocity for $\omega \to \infty$, negative branches. (b) Wave propagation velocity for $\omega \to 0$, negative branches.

Figure 7. Wave propagation velocity as a function of the F for fixed wavenumbers for a Herschel-Bulkley fluid, with $F_{min} = 0.18$.

Through the Fig. 7 it is possible to observe that, for $\omega \geq 1$, the variation of U occurs almost exclusively as function of F, as expected by Eq. 28. On the other hand, for $\omega < 1$, it is perceive that U assumes a dependency on ω, for $F < F_s$. In both cases, U will assume a constant value when $F \to \infty$. In fact, if we still consider that $F \to \infty$, then we have from Eq. (28) that

$$U(\omega \to 0) = \frac{1}{1 \pm \sqrt{1 - \frac{1}{\alpha}}}, \tag{29}$$

which still can be confirmed through Fig. 7. It is noting that this expression also present different dependency relation when compared to its analogous function in Eq. (20).

4. CONCLUSIONS

In the present work, a linear stability analysis was carried about the conservation equations of the fluid dynamic problem representative of a laminar flow over an inclined plane of a non-Newtonian fluid. The stability analysis was performed on the temporal and spatial evolution of the disturbances obtained from the solution of the characteristic dispersion equation of the problem.

A mathematical procedure was carried and provided criteria to evaluate the dynamic stability of the system. Those culminated in verifying the control parameters of the propagation of hydrodynamic instabilities. The results of the stability analysis were explored for a specific non-Newtonian fluid with parameters $n = 1/3$ and $C = 0.3$. The results of the stability analysis were explored by means of their asymptotic values for long waves ($k \to 0$) and short waves ($k \to \infty$).

The results of the temporal analysis showed that the temporal growth rate ($Im\{\omega_{\pm}(k)\}$) of disturbances strongly depends on the frequency of the perturbation and on the control parameter F, according with Liu (1994); Ng and Mei (1994); Maciel *et al.* (2013); Ferreira (2013). The results found here for this analysis corroborate those already developed in the literature, which present the existence of necessary condition $F = F_{min}$, so that the propagation of instabilities is amplified by the flow.

From Fig. 1 and results obtained by Eq. (15), (16) and (17), we concluded that it would be worth a discussion about the amplification and attenuation characteristics as a function of the wavenumber, since short waves amplify more quickly and long waves are normally those that stabilize in the flow (Zanuttigh and Lamberti, 2007). From a geometric analysis of the solution, limit values for growth and attenuation rates were sought, from where the minimum instability attenuation value was defined as ϑ, that is, function of the characteristics fluid rheology.

Based on the analysis of the wave propagation velocity, it was observed that U have a strong dependence on the wavenumber for small values of k. However, it was observed that for high wavenumber, U is constant, according to Fig. 2, dependent only on F. At the limit when $k \to 0$, it was noticed that the propagation velocity is independent of F. On the other hand, when $k \to \infty$, U depends only on F, given a specific fluid.

Thus, it is perceive that there must be a competition between the branches originated from the disturbance, and it would define which waves will be amplified: when does the growth rate of disturbances becomes irrelevant to their propagation? In other words, for what values for k is the growth rate strong enough to produce waves that will dominate the flow?

On the other hand, the results of the spatial linear stability analysis with regard to the spatial growth rate of instabilities ($Im\{k_{\pm}(\omega)\}$) showed the existence of a singularity point, F_s, which strongly contributes strongly to a change in the behavior of the instability growth rate. This singularity point require careful analysis when understanding the types of instability in propagation. The Fig. 5 graphically represents this statement, where $Im\{k_{+}(\omega)\}$ varies strongly with the passage through the singularity and shows a change from evanescence and amplification.

Finally, concerning the behavior of the propagation velocity function (Eq. (28)), the spatial stability analysis also showed that U for $F_{min} < F < F_s$ can have negative values, meaning that perturbations with velocity contrary to the flow could amplify, pointing to the coexistence of two waves in amplification in the domain. On the other hand, for $F > F_s$, agrees with the temporal analysis, showing that the two branches have positive values for.

5. ACKNOWLEDGEMENTS

The authors of the present paper is grateful to the Federal Institute Catarinense - Sombrio Advanced Campus for granting full time leave to study for a doctorate, via notice nº 21/2019.

6. REFERENCES

Balmforth, N.J. and Mandre, S., 2004. "Dynamics of roll waves". *Journal Fluid Mech*, Vol. 514, pp. 1–33.

Briggs, R.J., 1964. *Electrons-Stream Interaction with Plasmas*. MIT Press, Massachusetts.

Charru, F., 2011. *Hydrodynamic Instabilities*. Cambridge Texts in applied Mathematics, Cambridge.

Di Cristo, C., Iervolino, M., Vacca, A. and Zanuttigh, B., 2010. "Minimum channel length for roll-wave generation". *Journal of Hydraulic Research*, Vol. January 2008, pp. 73–79.

Di Cristo, C. and Vacca, A., 2005. "On the convective nature of roll waves instability". *Journal of Applied Mathematics*, Vol. 3, pp. 259–271.

Dressler, R.F., 1949. "Mathematical solution of the roll-waves in inclined open channels". *Communications on Pure and Aplied Mathematics*, Vol. 2, pp. 149–194.

Fer, I., Lemmin, U. and Thorpe, S., 2002. "Winter cascading of cold water in lake geneva". *Journal of Geophysical Research*, Vol. 107.

Ferreira, F.O., 2013. *Estabilidade e controle dinâmico de roll waves.* Doutorado em Engenharia Elétrica, Universidade Estadual Paulista - UNESP, Ilha Solteira/SP.

Fiorot, G.H., 2012. *Mitigação de riscos e catástrofes naturais: análise numérico-experimental de roll waves evoluindo em canais inclinados.* Mestrado em Engenharia Mecânica, Universidade Estadual Paulista - UNESP, Ilha Solteira/SP.

Huerre, P. and Monkewitz, P.A., 1990. "Local and global instabilities in spatially developing flows". *Annual Review of Fluid Mechanics*, Vol. 22, No. 1, pp. 473–537.

Ishihara, T., Iwagaki, Y. and Iwasa, Y., 1954. "Theory of roll waves trains in laminar water flow on a steep slope surface." *Transactions of the Japan Society of Civil Engineers*, Vol. 1954, No. 19, pp. 46–57.

Jeffreys, H., 1925. "LXXXIV. the flow of water in an inclined channel of rectangular section". *The London, Edinburgh, and Dublin Philosophical Magazine and Journal of Science*, Vol. 49, No. 293, pp. 793–807.

Liu, K.; Mei, C., 1994. "Roll waves on a layer of a muddy fluid flowing down a gentle slope – a bingham model." *Physics of Fluids*, Vol. 6, No. 8, pp. 2577–2589.

Maciel, G.F., Ferreira, F.O. and Fiorot, G.H., 2013. "Control of instabilities in non-newtonian free surface fluid flows". *Journal of the Brazilian Society of Mechanical Sciences and Engineering*.

Needham, D.J. and Merkin, H., 1984. "On roll waves down an open inclined channel". *Journal Mathematical Physical & Engineering Sciences*, Vol. 394, pp. 259–278.

Ng, C.O. and Mei, C.C., 1994. "Roll waves on a shallow layer of mud modelled as a power-law fluid". *Journal of Fluid Mechanics*, Vol. 263, p. 151–184.

Zanuttigh, B. and Lamberti, A., 2007. "Instability and surge development in debris flows". *Reviews of Geophysics*, Vol. 45, No. 3, pp. 1–45. ISSN 8755-1209. doi:10.1029/2005RG000175.

7. RESPONSIBILITY NOTICE

The authors are the only responsible for the printed material included in this paper.